Multifractal spectra of mean first-passage-time distributions in disordered chains

Pedro A. Pury*
Facultad de Matemática, Astronomía y Física, Universidad Nacional de Córdoba, Ciudad Universitaria, 5000 Córdoba, Argentina

Manuel O. Cáceres†
Centro Atómico Bariloche, Instituto Balseiro, and Consejo Nacional de Investigaciones Científicas y Técnicas, 8400 San Carlos de Bariloche, Río Negro, Argentina
(Received 24 February 2003; published 12 June 2003)

The multifractal characterization of the distribution over disorder of the mean first-passage time in a finite chain is revisited. Both, absorbing-absorbing and reflecting-absorbing boundaries are considered. Two models of dichotomic disorder are compared and our analysis clarifies the origin of the multifractality. The phenomenon is only present when the diffusion is anomalous.

DOI: 10.1103/PhysRevE.67.061106 PACS number(s): 05.40.Fb, 05.60.Cd, 89.75.Da, 02.50.Ng

I. INTRODUCTION

In the past two decades, a great effort has been devoted to the study of diffusion and transport in disordered media by models based on random walks [1–3]. Basically, the dynamics of the system can be described by a master equation for a particular probability distribution. Two alternative ways are usually employed. The first one is based on the probability $P(r,t)$ that the walker is on site r at time t when starting from the origin at $t=0$. The second way consists of analyzing the statistics of the exit time from a given region. In both cases, there are exact enumeration techniques which enable us to calculate the corresponding observable in all the possible disorder configurations. Thus, we can numerically reckon the distribution over disorder of the probability $P(r,t)$, or the moments $\langle P^q(r,t)\rangle$ of this distribution [3–9]. In an analogous manner, we can numerically evaluate the distribution of the mean first-passage time (MFPT) over disorder, or its moments [10–16],

$$M(q)=\int_0^\infty T^q \rho(T)\,dT, \tag{1}$$

where $\rho(T)$ is the distribution over disorder and q is a real number not necessarily integer. The crucial point of diffusion in disordered media is that transport can be *anomalous*, i.e., the mean square displacement of a random walk scales with time as $\langle r^2\rangle = Dt^{2/d_w}$, where $d_w>2$ is the anomalous diffusion exponent. A relevant property of the anomalous diffusion is that it leads to broad distributions. Their moments cannot be described by a single exponent but an infinite hierarchy of exponents is needed to characterize them [9,13]. This fact enables us to study the distributions over disorder with the multifractal formalism [17,18].

Random walks on random fractals (such as the infinite percolation cluster at criticality) are processes with anomalous diffusion, which are characterized by logarithmically broad distribution functions reflecting an underlying multifractal structure [3,4,6–8,10]. An important issue in these systems is the nature of the multifractality based on the dynamical process or in the steady state (as the voltage drop distribution in percolation). For the voltage drop distribution, the multifractal behavior is well established for all values of q [3]; whereas for the dynamical diffusive process the multifractality only appears in a range of values of q [8]. Another property of these processes is that while the multifractal behavior appears in the distribution of the probability $P(r,t)$, it is not present in the mean number of distinct sites visited by a particle diffusing on the percolating cluster [19]. Another dynamical process with ''ultra-anomalous'' slow motion is the Sinai model [20] for diffusion in a linear chain in the presence of random fields. For this model, the mean square displacement of a random walk follows asymptotically $\langle r^2\rangle \approx \ln^4 t$. Several studies [5,11,12,14,15,21] have established the multifractal properties of the model. However, the origin of the multifractality in this process is yet an open question.

In this work, we revisit the Sinai model and we address the last question. Particularly, we compare the behavior of the MFPT distributions over disorder and its moments for two processes with dichotomic disorder. One of them is the Sinai model and the other is a nonanomalous biased random walk in a finite disordered chain. The outline of the paper is as follows. In Sec. II, we present expressions for the MFPT for a given realization of the (quenched) disorder in the chain. The description of the models of disorder, employed in our studies, is given in Sec. III. The moments of the MFPT distribution over disorder diverge with the system's size. These divergences are characterized by the scaling exponents $\xi(q)$ in Sec. IV, where we employ the multifractal formalism [17,18] to calculate the exponents $\tau(q)$ of the corresponding partition function. Also, the generalized Renyi dimensions $D(q)$, and the spectra $f(\alpha)$ are given in that section. Finally, in Sec. V, we briefly summarize the results of our work.

II. MEAN FIRST-PASSAGE TIME IN QUENCHED DISORDERED CHAINS

We consider the continuous time dynamics of a random walk on a discrete one-dimensional lattice with nearest neighbor hopping. The walker jumps from site n to site n

*Electronic address: pury@famaf.unc.edu.ar
†Electronic address: caceres@cab.cnea.gov.ar

$+1$ with transition probability per unit time w_n^+, or to site $n-1$ with transition probability per unit time w_n^-. We are concerned with the exit time of the walker from the finite interval $D=[-M,L]$ on the chain, with at least one absorbing end. The average of the survival time until the absorption, over realizations of the random walk, is the MFPT. Recently, we have obtained a general exact expression for the MFPT for a fixed set of transition probabilities $\{w_j^{\pm}\}$ [22]. Let T_n denote the MFPT if the walker initially began at site $n \in D$. For an interval with both absorbing extremes ($w^+_{-(M+1)}=w^-_{L+1}=0$) we get

$$T_n=\frac{1+\sum_{k=-M}^{n-1}\prod_{j=-M}^{k}\frac{w_j^-}{w_j^+}}{1+\sum_{k=-M}^{L}\prod_{j=-M}^{k}\frac{w_j^-}{w_j^+}} \times\left(\sum_{k=-M}^{L}\frac{1}{w_k^+}+\sum_{k=-M}^{L-1}\frac{1}{w_k^+}\sum_{i=k+1}^{L}\prod_{j=k+1}^{i}\frac{w_j^-}{w_j^+}\right) -\left(\sum_{k=-M}^{n-1}\frac{1}{w_k^+}+\sum_{k=-M}^{n-2}\frac{1}{w_k^+}\sum_{i=k+1}^{n-1}\prod_{j=k+1}^{i}\frac{w_j^-}{w_j^+}\right). \quad (2)$$

In this work we fix the starting point $n=0$ (defining $T \equiv T_0$) and we consider two possible boundary conditions. The first one is the interval $[-L,L]$ with absorbing-absorbing (AA) extremes. The total number of sites, N_s, in the interval is $2L+1$. The MFPT for this case is given by Eq. (2) taking $M=L$. The second case is the interval $[0,L]$ with reflecting-absorbing (RA) ends. Here, $N_s=L+1$ and from Eq. (2), taking $n=0$, $M=0$, and $w_0^-=0$, we immediately obtain for the MFPT [22],

$$T=\sum_{k=0}^{L}\frac{1}{w_k^+}+\sum_{k=0}^{L-1}\frac{1}{w_k^+}\sum_{i=k+1}^{L}\prod_{j=k+1}^{i}\frac{w_j^-}{w_j^+}. \quad (3)$$

The effect of the reflecting boundary is the striking simplification of the structure of the equation for the MFPT. This fact leads us to consider also the AA boundary conditions in the problem of multifractality of the MFPT distribution over disorder.

In finite discrete systems, we can enumerate all the configurations $\mathcal{N}$ of disorder. We denote by $T_{(i)}$ the MFPT for the ith realization of the quenched disorder. We stress that all the configurations of disorder are equally probable. However, the resulting values $T_{(i)}$ are distributed by $\rho(T)$, the MFPT distribution over disorder. Thus, we can compute exactly the moments of the MFPT distribution, given the set of values $\{T_{(i)},\ i=1,\ldots,\mathcal{N}\}$, from the definition given by Eq. (1),

$$M(q)\equiv\frac{1}{\mathcal{N}}\sum_{i=1}^{\mathcal{N}}T_{(i)}^q. \quad (4)$$

In particular, the MFPT averaged over disorder results in $M(1)$. For dichotomic models of disorder, in a chain with N_s sites, there are $\mathcal{N}=2^{N_s}$ possible realizations of the random lattice, which can be easily enumerated. The set of values $\{T_{(i)},\ i=1,\ldots,\mathcal{N}\}$ can be exactly calculated employing expression (2) for the AA boundary conditions, or by Eq. (3) for the RA extremes.

III. MODELS OF DISORDERED CHAINS

Now, we assume that the hopping probabilities $w_j^{\pm}$ are strictly positive random variables, chosen independently from site to site and identically distributed. Additionaly, we admit that the site transition probabilities are not necessarily symmetric in the sense that $w_j^+ \neq w_j^-$. Thus, we can incorporate the effects of bias in to the chain by external fields.

We select the first distribution for the transition probabilities in such a way that they satisfy the Sinai condition [20], namely, the random variable $\ln(w_j^+/w_j^-)$ has zero mean and finite variance σ^2. Thus, we consider a dichotomic model by defining $w_j^-=1-w_j^+$ and prescribing w_j^+ to be equal to $1/2\pm\epsilon$ with equal probabilities. The parameter ϵ measures the strength of disorder, and can take values between 0 and 1/2. $\epsilon=0$ corresponds to a simple homogeneous random walk, and for $\epsilon>0$ we get a disordered random walk with local bias (random field). It is easily verified that the above prescriptions satisfy the Sinai condition. Particularly, we obtain $\sigma^2=\ln^2\gamma(\epsilon)$, where $\gamma(\epsilon)\equiv(1+2\epsilon)/(1-2\epsilon)$. In the asymptotic limit $\epsilon\to 1/2$, the variance diverges. The MFPT averaged over disorder for the dichotomic Sinai model diverges as $\beta(\epsilon)^{N_s}$ for $N_s\to\infty$, where $\beta(\epsilon)\equiv(1+4\epsilon)/(1-4\epsilon)$ [23], whereas the typical value of the first-passage time, defined as $\exp(\langle \ln T\rangle)$, diverges slower, as $\exp(\sigma\sqrt{\pi N_s/2})$ [24]. Here, the brackets $\langle\cdots\rangle$ denote the average over the disorder. Therefore, the distribution of the MFPT over the Sinai disorder has a power-law tail [25].

It is easily seen that the largest value of the MFPT, $T_{\max}$, is obtained for the RA ends when at all the sites, the right jump transition is $1/2-\epsilon$, and the left jump transition is $1/2+\epsilon$. In the asymptotic limit of $N_s\to\infty$, we obtain $T_{\max}\approx\gamma^{N_s}$ [14]. For the AA extremes, $T_{\max}$ cannot be easily evaluated. Thus, instead of an analytical expression, in Fig. 1 we show a numerical calculation of $T_{\max}$ for several values of ϵ. We see that asymptotically $\log(T_{\max})\approx N_s$, as in the RA case.

In Fig. 2, we show the histogram of the distribution $\rho(T)$ over the dichotomic Sinai disorder. The figure was constructed computing Eq. (2) for $M=L=7$ ($N_s=15$), and using all the possible configurations of disorder. A related figure, for the histogram of $\rho(T)$ for chains with the RA extremes, can be seen in Ref. [14]. The distribution $\rho(T)$ has previously been studied [25] for the RA boundary conditions and results broad.

Our second random biased model for the transition probabilities is defined by $w_j^-=w_j^+-\epsilon$ and prescribing w_j^+ to be equal to 1/2 or 3/2 with equal probabilities. In this case, the parameter ϵ measures the strength of the bias, and can take values between 0 and 1/2. In the limit of $\epsilon=0$, we get a disordered symmetrical random walk. This dichotomic model corresponds to a class of weak disorder with global bias. The quantities $\beta_k\equiv\langle(1/w_j^+)^k\rangle$ result finite for all $k \geqslant 1$. Therefore, the model does not present anomalous diffu-

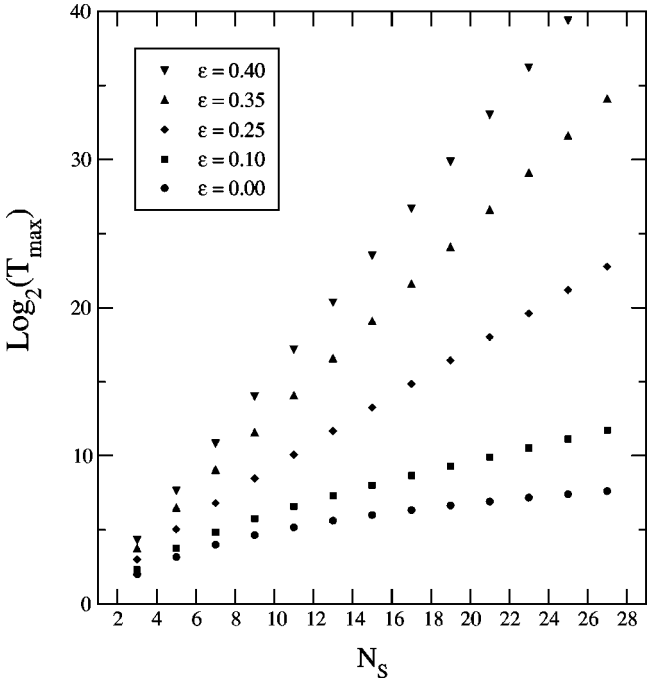

FIG. 1. Numerical evaluation of $T_{\max}$ as a function of N_s for chains with the AA ends and L from 1 to 13.

sion [1]. For the MFPT averaged over disorder with the AA boundary conditions, we obtain up to first order in ϵ [22,26],

$$M(1) \simeq \frac{(L+1)^2}{2\beta_1^{-1}}\left[1+\frac{1}{2}(1+\mathcal{F})\beta_1\epsilon\right]. \tag{5}$$

The asymmetry in the hopping transitions links the strength of the bias with the fluctuation of the disorder, defined by $\mathcal{F}\equiv(\beta_2-\beta_1^2)/\beta_1^2$. In our particular case, we get $\beta_1=4/3$, and $\mathcal{F}=1/4$. On the other hand, for the RA extremes, we obtain up to first order in ϵ [22],

$$M(1) \simeq \frac{(L+1)(L+2)}{2\beta_1^{-1}}\left[1-\frac{L}{3}\beta_1\epsilon\right]. \tag{6}$$

Strikingly, for these boundary conditions, the fluctuation of the disorder is not present in the averaged MFPT. This fact relies on the difference in the structures of Eqs. (2) and (3). In the limit of $L\to\infty$, $M(1)$ diverges as L^2 independently of the boundary conditions.

In Fig. 3, we show the histogram of the corresponding distribution $\rho(T)$ over dichotomic weak disorder. Here, we do not obtain a broad but a more localized distribution. We must stress the difference in the scales used to construct the plots in Figs. 2 and 3. This fact is the first indication of the different nature in the distribution over disorder between both models. Both models were constructed to get $\langle w_j^+\rangle = 1$, and the main difference among them is in the role of the parameter ϵ. This parameter controls the disorder in the Sinai model and regulates the bias in the second model. Thus, in the Sinai model the bias is local, i.e., the direction of the bias is randomly drawn in each site, whereas in the second model, we are considering a global bias field which points to the right in all sites. Assuming that the jump probabilities per unit time involve the Arrhenius factor (see Ref. [26]), the landscape for the particle potential is schematically sketched in Fig. 4 for both models.

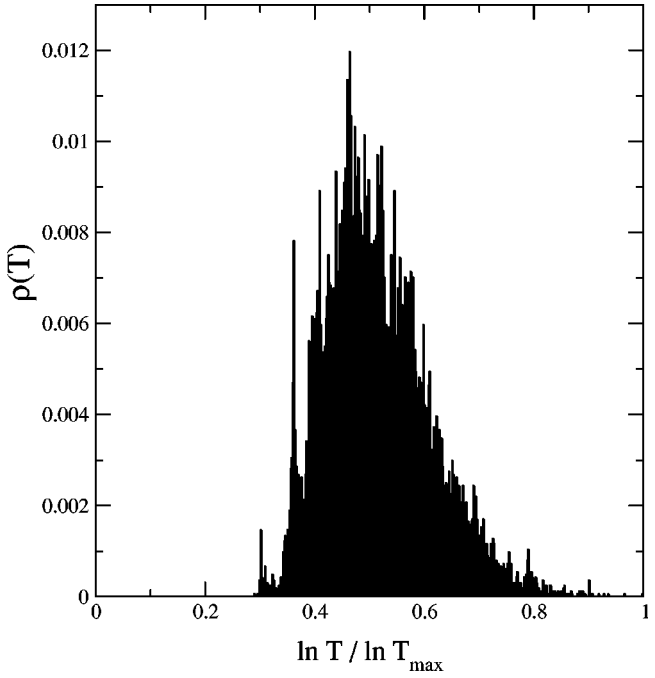

FIG. 2. Histogram of $\rho(T)$ for a chain with $L=7$, the AA boundary conditions, and the Sinai disorder with $\epsilon=0.25$. We are using the rescaled variable $\ln T/\ln T_{\max}$ and uniform buckets of width equal to 2^9. $T_{\max}=9824$.

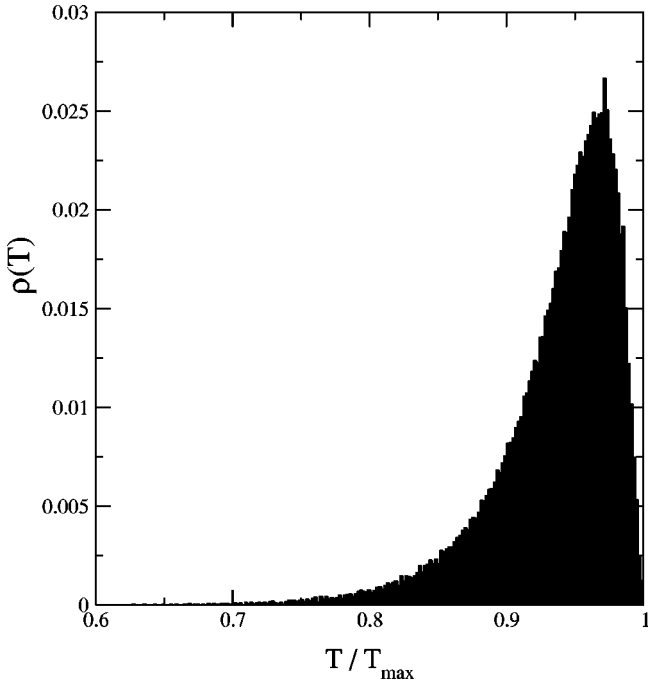

FIG. 3. Histogram of $\rho(T)$ for a chain with $L=7$, the AA boundary conditions, and weak disorder with $\epsilon=0.25$. We are using uniform intervals of width equal to 2^9. $T_{\max}=31.75$.

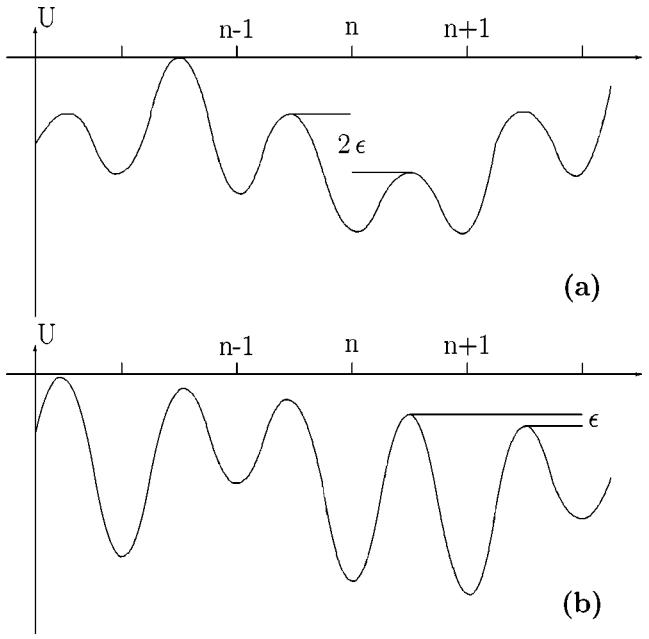

FIG. 4. Sketches of the particle potential for both kinds of disorder and small ϵ: (a) The Sinai model. The difference between two consecutive peaks is 2ϵ, with random sign. (b) Weak disorder. The difference between one peak and the following is always ϵ.

IV. MULTIFRACTAL ANALYSIS

In order to characterize the divergences of the moments of the MFPT distribution over disorder, we postulate that in the limit $N_s \to \infty$, the qth moment obeys the scaling relation $M(q) \sim \mathcal{N}^{\xi(q)}$. In order to verify this ansatz, we have numerically reckoned $\log[M(q)]$ vs N_s. For chains with the AA ends, we take L from 1 to 13 and use Eq. (2) for evaluating the set $\{T_{(i)}, i=1, \ldots, \mathcal{N}\}$, for a given L. For chains with the RA boundary conditions, we take L from 1 to 20 and use Eq. (3) for calculating the values $T_{(i)}$, for a fixed size of the chain. For all values of ϵ and q, and for both models of disorder, with the AA or RA extremes, we obtain straight lines.

The slope of the linear fitting for the Sinai model with the AA (RA) ends is plotted in Fig. 5 (Fig. 6) as functions of q, for three values of ϵ. For all ϵ, we obtain that $\xi(q)$ is a monotonically increasing function with $\xi(0)=0$, which is due to the normalization condition of the distribution. We observe that for large values of ϵ, $\xi(q)$ is a nonlinear function; whereas in the limit of weak disorder, $\xi(q)$ becomes a linear function. For the model of weak disorder, we obtain $\xi(q)=\theta q$, where $\theta>0$ is a decreasing function of ϵ. Therefore, for weak disorder, we get a single gap exponent for describing the moments of the MFPT distribution. The analysis with both kinds of boundary conditions leads us to qualitatively similar behaviors for the exponents $\xi(q)$, for both models of disorder described in Sec. III.

Now, let us define the partition function as follows [17]:

$$Z(q) = \frac{1}{\left(\sum_{i=1}^{\mathcal{N}} T_{(i)} \right)^q} \sum_{i=1}^{\mathcal{N}} T_{(i)}^q . \tag{7}$$

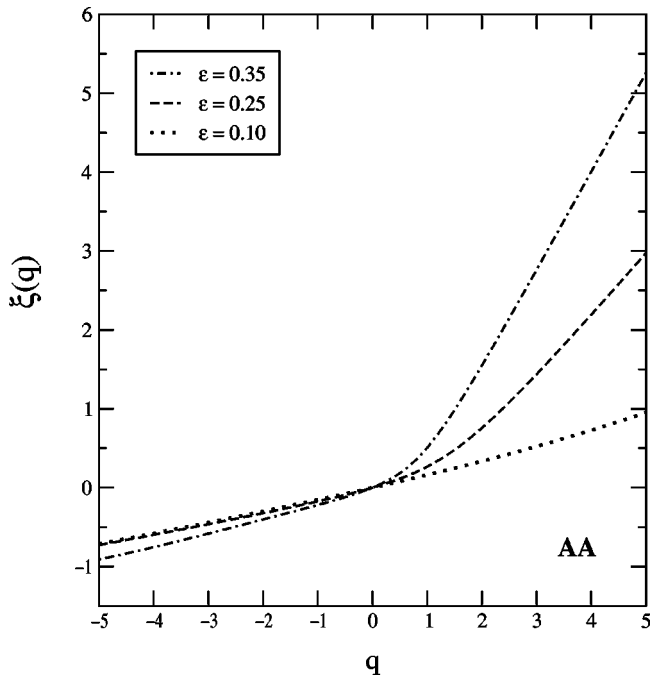

FIG. 5. Plot of the scaling exponents $\xi(q)$ for chains with the AA boundary conditions and the Sinai disorder.

Again, we postulate that in the limit $N_s \to \infty$, the partition function obeys a scaling relation. Thus, we write $Z(q) \sim \mathcal{N}^{-\tau(q)}$. It is well known that for nonmultifractal distributions, the exponents $\tau(q)$ are linear functions on q, namely, $\tau(q)=q-1$. The multifractality appears with a nontrivial dependence of the scaling exponents on q. For all values of ϵ and q, and for both models of disorder, we obtain straight lines when we plot $\log[Z(q)]$ vs N_s. Therefore, the scaling

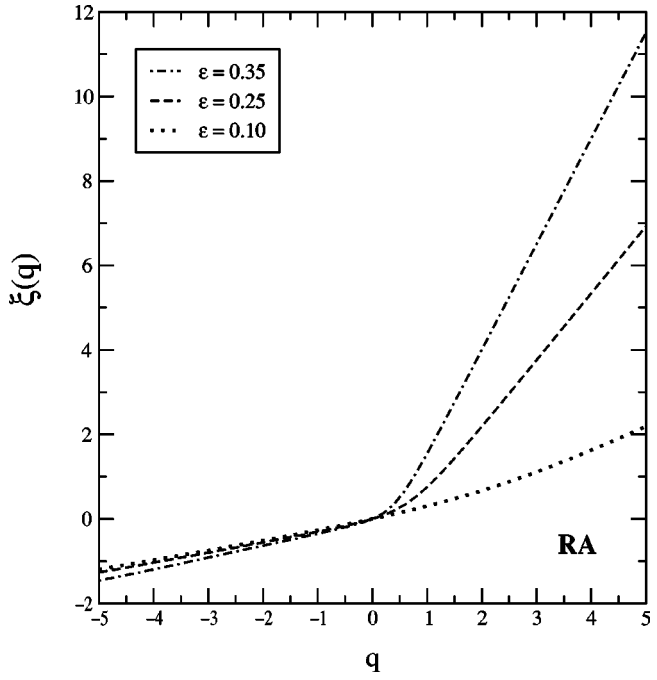

FIG. 6. Plot of the scaling exponents $\xi(q)$ for chains with the RA boundary conditions and the Sinai disorder.

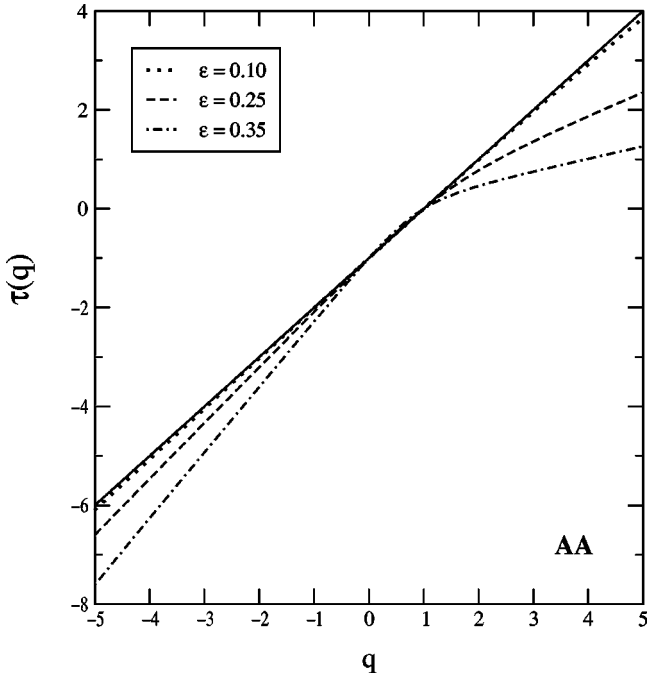

FIG. 7. Plot of the scaling exponents $\tau(q)$ for chains with the AA boundary conditions and the Sinai disorder, using L from 5 to 13. The solid line corresponds to the linear relation $q-1$.

ansatz is verified. Here, we have also used L from 1 to 13 for the AA ends, and L from 1 to 20 for the RA extremes.

In Fig. 7 (Fig. 8), we plot $\tau(q)$ for chains with the dichotomous Sinai model, the AA (RA) ends, and for three representative values of ϵ. The functions $\tau(q)$ satisfy $\tau(0)=-1$. Additionally, we get $\tau(1)=0$, which is due to the

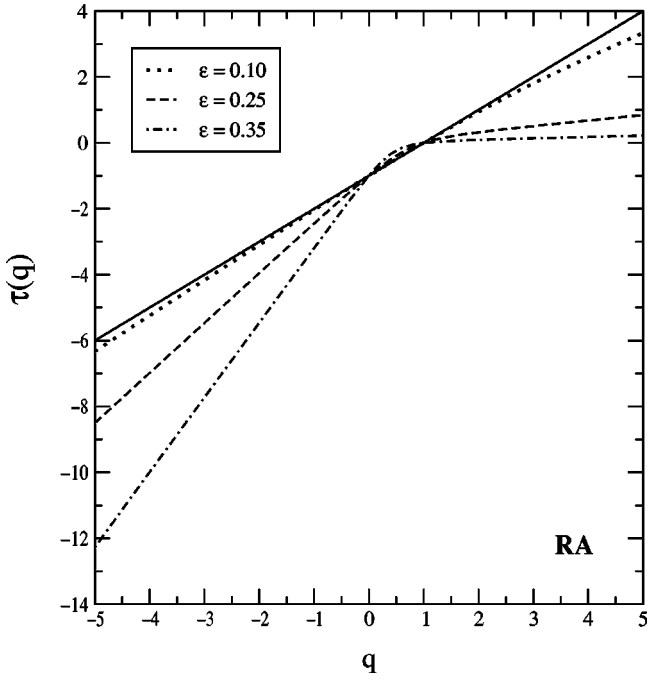

FIG. 8. Plot of the scaling exponents $\tau(q)$ for chains with the RA boundary conditions and the Sinai disorder, using L from 6 to 14. The solid line corresponds to the linear relation $q-1$.

TABLE I. Fitted values for the parameters p_1 and p_2, using Eq. (8), for the plots $\tau(q)$ in Figs. 7 and 8.

	AA		RA	
ϵ	p_1	p_2	p_1	p_2
0.00	0.500	0.500	0.500	0.500
0.10	0.461	0.543	0.425	0.602
0.25	0.395	0.700	0.295	0.878
0.35	0.336	0.825	0.173	0.964

normalization condition of $Z(q)$. In the limit of $\epsilon\to 0$, $\tau(q)\approx q-1$, and for strong disorder, $\tau(q)$ exhibits a nonlinear dependence. Thus, the multifractality for the Sinai model is unambiguously established, independently of the boundary conditions. For the model of weak disorder, we obtain $\tau(q)=q-1$ for all values of ϵ, within the accuracy of the numerical evaluations. Therefore, we have not found multifractality in our model of weak disorder, neither with the AA nor with the RA boundary conditions. This result reinforces the idea that the multifractal phenomenon is only related to anomalous diffusion. Both models are based on the same dichotomic rule for assigning values to the transition probabilities. Moreover, in both cases we found $\langle w_j^+\rangle=1$. In spite of these similar characteristics, the selected models have quite different behaviors. The random field resulting from the Sinai condition is at the basis of the anomalous diffusion and the origin of the multifractal behavior of the MFPT distribution over disorder.

The simple plots obtained in the graphs for the functions $\tau(q)$ suggest us that the multifractality is due to the presence of a binomial multiplicative process. For this process, the mass exponents are [18]

$$\tau(q)=-\frac{\ln(p_1^q+p_2^q)}{\ln 2}, \tag{8}$$

where $p_1+p_2=1$. This expression immediately satisfies the conditions $\tau(0)=-1$ and $\tau(1)=0$, and in the limit $p_1=p_2=1/2$, results in $\tau(q)=q-1$. For $p_1<1/2$, we get the limit expressions

$$\tau(q)\to -q\frac{\ln p_1}{\ln 2} \quad \text{for } q\to-\infty, \tag{9}$$

$$\tau(q)\to -q\frac{\ln p_2}{\ln 2} \quad \text{for } q\to\infty. \tag{10}$$

In our case, the parameters p_1 and p_2 are functions of the strength of disorder (ϵ). In Table I, the values of the fitting of $\tau(q)$, using the two parameters p_1 and p_2, are displayed for both kinds of boundary conditions. We only obtain a good quality of fitting for small values of ϵ. For strong disorder, the condition $p_1+p_2=1$ is relaxed and we can only fit both asymptotic regimes of the curves for $q\to\pm\infty$. This fact is a strong indication that the nature of the multifractal phenomenon is more complex than a multiplicative rule.

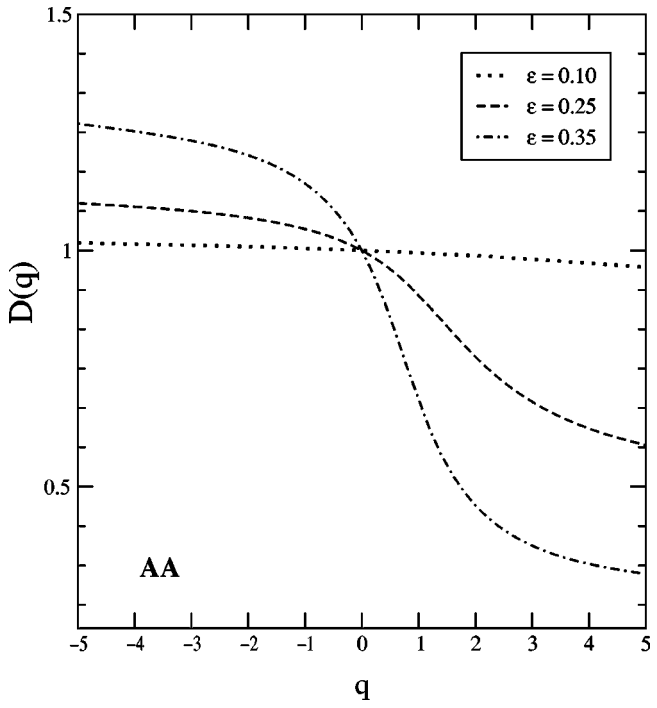

FIG. 9. Generalized dimensions $D(q)$ for chains with the AA boundary conditions and the Sinai disorder.

A usual characterization of multifractality is the generalized Renyi dimension spectrum [18] defined by [27]

$$D(q) \equiv \frac{\tau(q)}{q-1}. \tag{11}$$

In Fig. 9 (Fig. 10), we depict the generalized dimension spectra for the same conditions and values of ϵ as given by Fig. 7 (Fig. 8). We find that $D(q)$ is a monotonically decreasing function of q, and satisfies $D(0)=1$, which is the dimension of the support of the distribution.

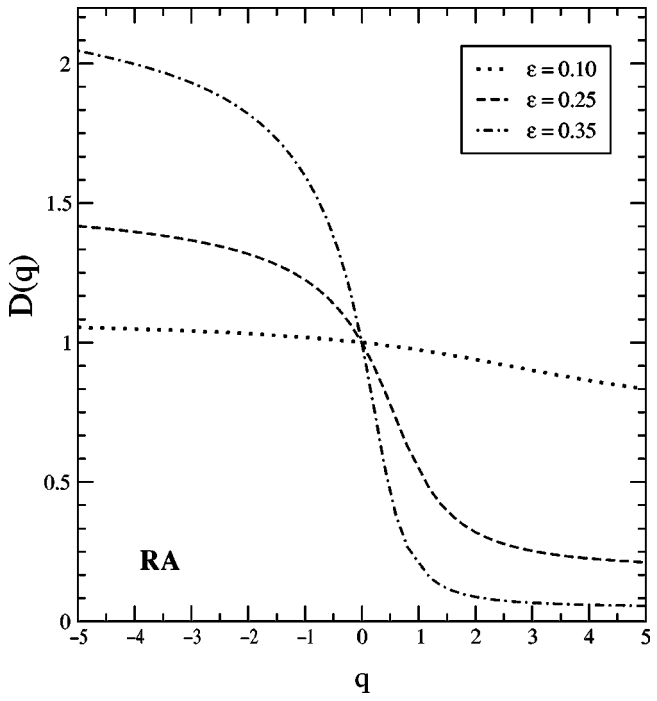

FIG. 10. Generalized dimensions $D(q)$ for chains with the RA boundary conditions and the Sinai disorder.

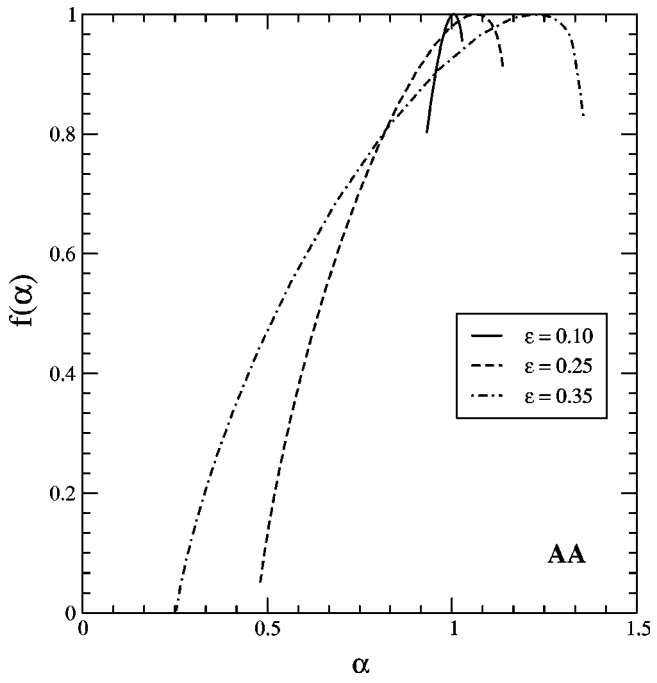

FIG. 11. Multifractal spectra $f(\alpha)$ for chains with the AA boundary conditions and the Sinai disorder.

Taking the Legendre transform of $\tau(q)$, we can obtain the multifractal spectrum $f(\alpha)=-\tau(q)+q\alpha$, where the Lipschitz-Hölder exponent α is the derivative of $\tau(q)$ with respect to q. Figure 11 (Fig. 12) shows the $f(\alpha)$ spectra for

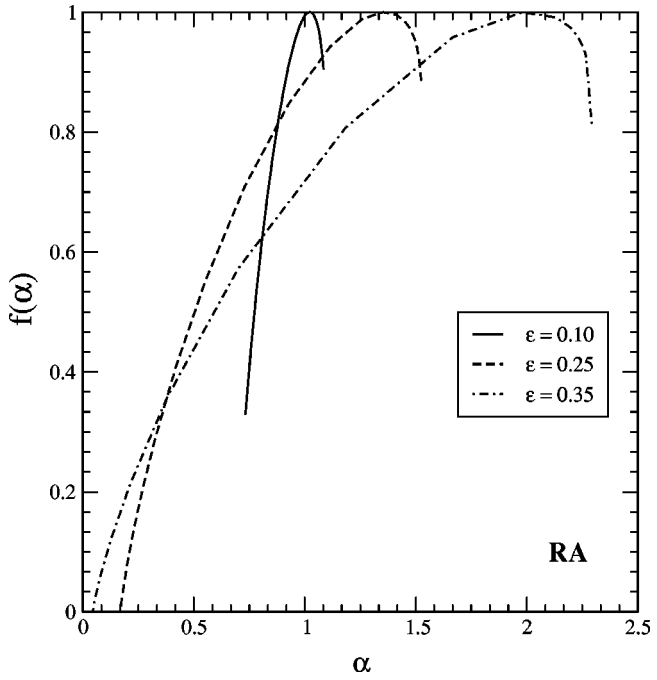

FIG. 12. Multifractal spectra $f(\alpha)$ for chains with the RA boundary conditions and the Sinai disorder.

the same conditions and values of ϵ as given by Fig. 7 (Fig. 8). For strong disorder, the curve $f(\alpha)$ becomes broad, whereas for $\epsilon \to 0$ the spectrum collapses to the point (1,1). As is known, the maximum value of f is the fractal dimension of the support of the measure.

In this work, we have chosen the scaling parameter $\mathcal{N}$ to characterize the system size. In Ref. [14], a similar multifractal analysis for the Sinai disorder and the RA boundary conditions was based on the scaling parameter $T_{\max}$. We have seen in Sec. III that $T_{\max} \propto \mathcal{N}$. However, this choice of the scaling parameter leads to spurious results, such as the variation of $D(0)$ with ϵ. This phenomenon is an artifact of the mathematical selection of the scaling parameter, and not a characteristic property of the system under analysis. On the other hand, for one-dimensional systems, we expect that the dimension of the support of the multifractal measure is equal to 1.

Finally, we derive the relation between the exponents $\xi(q)$ and $\tau(q)$. From the definitions given by Eqs. (4) and (7), we inmediatly obtain

$$Z(q) = \frac{\mathcal{N}^{1-q}}{M(1)^q} M(q). \tag{12}$$

Using the scaling ansatz in the last equation and taking logarithms, we get

$$\tau(q) = q - 1 - \xi(q) + q\,\xi(1). \tag{13}$$

Particularly, the last relation satisfies inmediately that $\tau(0) = -1$ and $\tau(1) = 0$. From the result quoted in Sec. III, for chains with the RA ends, we found $\xi(1) = \log_2 \beta(\epsilon)$.

V. CONCLUDING REMARKS

In this work, we have considered the distribution of the MFPT over two classes of disorder, the Sinai and another dichotomic model with global bias and nonanomalous diffusion. Our results confirm us that the multifractality is related only to anomalous diffusion.

The multifractal behavior in the MFPT distribution over the Sinai disorder is not a consequence of the multiplicative structure of Eq. (2) or (3) (the expressions for the MFPT for a fixed realization of disorder), as was stated in a previous report [14]. The multifractality is an inherent attribute of the strong disorder in the Sinai model, and is well established for both kinds of boundary conditions. Moreover, the multifractal signature found in the spectra obtained suggests us that the origin of the phenomenon is more complex than a binomial multiplicative process.

ACKNOWLEDGMENTS

This work was partially supported by a grant from ''Secretaría de Ciencia y Tecnología de la Universidad Nacional de Córdoba'' (Code: 05/B160, Res. SeCyT 194/00). P.A.P. thanks Centro Atómico Bariloche for its hospitality during his stay. P.A.P. is also grateful to Peter Pfeifer for a useful discussion.

[1] S. Alexander, J. Bernasconi, W.R. Schneider, and R. Orbach, Rev. Mod. Phys. **53**, 175 (1981).
[2] J.W. Haus and K.W. Kehr, Phys. Rep. **150**, 263 (1987); S. Havlin and D. Ben-Avraham, Adv. Phys. **36**, 695 (1987); J.P. Bouchaud and A. Georges, Phys. Rep. **195**, 127 (1990).
[3] S. Havlin and A. Bunde, in *Fractals and Disordered Systems*, edited by A. Bunde and S. Havlin (Springer-Verlag, Berlin, 1991), Chap. 3.
[4] A. Bunde, H. Harder, S. Havlin, and H.E. Roman, J. Phys. A **20**, L865 (1987).
[5] H.E. Roman, A. Bunde, and S. Havlin, Phys. Rev. A **38**, 2185 (1988).
[6] A. Bunde, S. Havlin, and H.E. Roman, Phys. Rev. A **42**, 6274 (1990).
[7] H.E. Roman, Physica A **191**, 379 (1992).
[8] E. Eisenberg, A. Bunde, S. Havlin, and H.E. Roman, Phys. Rev. E **47**, 2333 (1993).
[9] E. Eisenberg, S. Havlin, and G.H. Weiss, Phys. Rev. Lett. **72**, 2827 (1994).
[10] N. Mašić and Z.V. Djordjević, Physica A **167**, 560 (1990).
[11] C. Van den Broeck, J. Stat. Phys. **65**, 971 (1991).
[12] K.P.N. Murthy, S. Rajasekar, and K.W. Kehr, J. Phys. A **27**, L107 (1994).
[13] T. Wichmann, A. Giacometti, and K.P.N. Murthy, Phys. Rev. E **52**, 481 (1995).
[14] K.P.N. Murthy, K.W. Kehr, and A. Giacometti, Phys. Rev. E **53**, 444 (1996).
[15] K.P.N. Murthy, A. Giacometti, and K.W. Kehr, Physica A **224**, 232 (1996).
[16] K. Kim, J.S. Choi, and Y.S. Kong, J. Phys. Soc. Jpn. **67**, 1583 (1998); K. Kim, G.H. Kim, and Y.S. Kong, Fractals **8**, 181 (2000).
[17] T.C. Halsey, M.H. Jensen, L.P. Kadanoff, I. Procaccia, and B.I. Shraiman, Phys. Rev. A **33**, 1141 (1986).
[18] J. Feder, *Fractals* (Plenum, New York, 1988).
[19] L.K. Gallos, P. Argyrakis, and K.W. Kehr, Phys. Rev. E **52**, 1520 (1995); K.P.N. Murthy, L.K. Gallos, P. Argyrakis, and K.W. Kehr, *ibid.* **54**, 6922 (1996).
[20] Y.G. Sinai, Theor. Probab. Appl. **27**, 256 (1982).
[21] R. Harisha and K. Murthy, Physica A **287**, 161 (2000).
[22] P.A. Pury and M.O. Cáceres, J. Phys. A **36**, 2695 (2003).
[23] K.P.N. Murthy and K.W. Kehr, Phys. Rev. A **40**, 2082 (1989); **41**, 1160(E) (1990).
[24] S.H. Noskowicz and I. Goldhirsch, Phys. Rev. Lett. **61**, 500 (1988).
[25] K.W. Kehr and K.P.N. Murthy, Phys. Rev. A **41**, 5728 (1990); S.H. Noskowicz and I. Goldhirsch, *ibid.* **42**, 2047 (1990).
[26] P.A. Pury and M.O. Cáceres, Phys. Rev. E **66**, 021112 (2002).
[27] Note that our definition of $\tau(q)$ is equal to minus the mass exponents used in Ref. [18]. Usually, the mass exponents are defined in the limit of a scaling parameter going to zero. In our case, the scaling relations hold for the parameter $\mathcal{N} \to \infty$. Therefore, we use the denominator $(q-1)$ in the definition of $D(q)$.